Title

Weighted average of shared trajectory: A new estimator for dynamic functional connectivity efficiently estimates both rapid and slow changes over time.

Authors

Faghiri, Ashkan
Iraji, Armin
Damaraju, Eswar
et al.

Publication Date

2020

DOI

10.1016/j.jneumeth.2020.108600

Peer reviewed

HHS Public Access

Author manuscript

J Neurosci Methods. Author manuscript; available in PMC 2021 July 21.

Published in final edited form as:

J Neurosci Methods. ; 334: 108600. doi:10.1016/j.jneumeth.2020.108600.

Weighted average of shared trajectory: a new estimator for dynamic functional connectivity efficiently estimates both rapid and slow changes over time

Ashkan Faghiri[a,b,l], **Armin Iraji**[a,l], **Eswar Damaraju**[a,l], **Aysenil Belger**[c,l], **Judy Ford**[d,e,l], **Daniel Mathalon**[d,e,l], **Sarah Mcewen**[f,l], **Bryon Mueller**[g,l], **Godfrey Pearlson**[h,l], **Adrian Preda**[i,l], **Jessica Turner**[j,l], **Jatin G. Vaidya**[k,l], **Theo G.M. Van Erp**[m,n], **Vince D. Calhoun**[a,b,j,l]

[a]The Mind Research Network, 1101 Yale Blvd NE, Albuquerque, NM, 87106, USA

[b]Electrical and Computer Engineering Department, University of New Mexico, Albuquerque, NM, USA

[c]Department of Psychiatry, University of North Carolina, Chapel Hill, NC, USA

[d]Department of Psychiatry, University of California San Francisco, San Francisco, CA, USA

[e]San Francisco VA Medical Center, San Francisco, CA, USA

[f]Department of Psychiatry and Biobehavioral Sciences, University of California Los Angeles, Los Angeles, CA, USA

[g]Department of Psychiatry, University of Minnesota, Minneapolis, MN, USA

[h]Yale University, School of Medicine, New Haven, CT, USA

[i]Department of Psychiatry and Human Behavior, University of California Irvine, Irvine, CA, USA

[j]Department of Psychology, Georgia State University, GA, USA

[k]Department of Psychiatry, University of Iowa, IA, USA

[l]Department of ECE, University of New Mexico, NM, USA

[m]Clinical Translational Neuroscience Laboratory, Department of Psychiatry and Human Behavior, University of California Irvine, 5251 California Ave, Irvine, CA, 92617, USA

[n]Center for the Neurobiology of Learning and Memory, University of California Irvine, 309 Qureshey Research Lab, Irvine, CA, 92697, USA

Abstract

Background—Dynamic functional network connectivity (dFNC) of the brain has attracted considerable attention recently. Many approaches have been suggested to study dFNC with sliding

Conflicts of interest

Authors declare no conflict of interests.

window Pearson correlation (SWPC) being the most well-known. SWPC needs a relatively large sample size to reach a robust estimation but using large window sizes prevents us to detect rapid changes in dFNC.

New method—Here we first calculate the gradients of each time series pair and use the magnitude of these gradients to calculate weighted average of shared trajectory (WAST) as a new estimator for dFNC.

Results—Using WAST to compare healthy control and schizophrenia patients using a large dataset, we show disconnectivity between different regions associated with schizophrenia. In addition, WAST results reveals patients with schizophrenia stay longer in a connectivity state with negative connectivity between motor and sensory regions than do healthy controls.

Comparison with Existing Methods—We compare WAST with SWPC and multiplication of temporal derivatives (MTD) using different simulation scenarios. We show that WAST enables us to detect very rapid changes in dFNC (undetected by SWPC) while MTD performance is generally lower.

Conclusions—As large window sizes are unable to detect short states, using shorter window size is desirable if the estimator is robust enough. We provide evidence that WAST requires fewer samples (compared to SWPC) to reach a robust estimation. As a result, we were able to identify rapidly varying dFNC patterns undetected by SWPC while still being able to robustly estimate slower dFNC patterns.

Keywords

functional magnetic resonance imaging; fMRI; brain dynamics; ICA; resting state; phase; shared trajectory; dynamic functional network connectivity

Introduction

Dynamic brain functional connectivity is currently a major focus in the neuroimaging field. The idea is that brain connectivity may not always be static and unchanging during the scan length (Allen, Damaraju, Plis, Erhardt, & … 2014; Hutchison, Womelsdorf, Allen, et al., 2013). Several methods have been proposed and applied to study dynamic functional connectivity between regions (dynamic functional connectivity; dFC) or between networks (dynamic functional network connectivity; dFNC). Methods developed to study dynamic connectivity include hidden Markov models (Ou et al., 2013), coactivation patterns using clustering approaches (Liu & Duyn, 2013) and windowless dictionary learning (Yaesoubi, Adali, & Calhoun, 2018). One method that shares some similarities to the method we propose here is called the multiplication of temporal derivatives (MTD;(Shine et al., 2015)). As we elaborate in the discussion section, the similarity between MTD and our proposed method is only in the use of derivatives. However, our approach uses them in a different way which we also believe provides more intuitive and graphically interpretable results.

The most widely used method to study dFNC utilizes a sliding window to calculate Pearson correlation (SWPC) (E. A. Allen et al., 2014; Chang & Glover, 2010; Hutchison, Womelsdorf, Gati, Everling, & Menon, 2013). This method has resulted in a considerable

number of interesting new findings for different brain related questions, but it has several shortcomings (Hutchison, Womelsdorf, Allen, et al., 2013). One problem with SWPC is that to reach a good estimation for Pearson correlation we need a relatively large number of samples. This forces us to use window size larger than a specific length which can result in loss of information if the change in FNC is fast relative to the length of the selected window (Leonardi & Van De Ville, 2015).

Here we introduce a new estimator for dFNC which we call weighted average of shared trajectory (WAST). We show that WAST, compared to SWPC, requires fewer samples to robustly estimate dFNC. This allows us to use smaller window sizes and therefore faster changes can be detected. To demonstrate the utility of our proposed method, we compare it to SWPC and MTD (another method that aims to estimate time-varying connectivity at a more rapid time resolution compared to SWPC) using simulated data. Finally, we employed WAST to analyze a real resting state fMRI dataset including healthy controls and patients with schizophrenia. The dataset we used has been studied extensively in earlier works (Damaraju et al., 2014; Hare et al., 2019; Yaesoubi et al., 2017).

We first motivate and introduce WAST. Next MTD is introduced briefly and simulation procedures are explained. These simulations are designed in such a way to allows us study WAST and its properties within known scenarios and compare it to SWPC and MTD. Finally, we introduce the fMRI dataset used in this study and analyze it using both WAST and SWPC estimators and draw conclusions about the results.

Methods

Using trajectory as a connectivity metric

In this section, we introduce WAST, a robust functional connectivity estimator. Assume we have two time series labeled $x_i(t)$ and $x_j(t)$. We can define a new space unique to these two time series in which our time series pair at time t will occupy a location at coordinate $[x_i(t), x_j(t)]$. At each time point we can estimate the gradient $\nabla_{x_i,x_j}(t)$.

$$\nabla_{x_i,\,x_j}(t) = \begin{bmatrix} x_i(t) - x_i(t-1) \\ x_j(t) - x_j(t-1) \end{bmatrix} \tag{1}$$

These gradients can show the trajectory shared between the two time series (i.e. $x_i(t)$ and $x_j(t)$) in the new defined space. As $\nabla_{x_i,x_j}(t)$ is essentially a vector it can be specified using its angle and magnitude:

$$\angle \nabla_{x_i,\,x_j}(t) = \tan^{-1} \frac{[x_i(t) - x_i(t-1)]}{[x_j(t) - x_j(t-1)]}$$

$$\left|\nabla_{x_i,\,x_j}(t)\right| = \sqrt{[x_i(t) - x_i(t-1)]^2 + \left[x_j(t) - x_j(t-1)\right]^2}$$

Figure 1 illustrate a graphical presentation for angle and magnitude of the gradients as defined above.

It can be seen that $\angle\nabla_{x_i,x_j}(t)$ is not equal to $\angle\nabla_{x_j,x_i}(t)$. Therefore, its value depends on the time series chosen to act as the horizontal axis. To remedy this issue, we modify its value:

$$\angle\nabla_{x_i,x_j}(t) = \begin{cases} \angle\nabla_{x_i,x_j}(t) & \left|\angle\nabla_{x_i,x_j}(t)\right| < \left|\angle\nabla_{x_j,x_i}(t)\right| \\ \angle\nabla_{x_j,x_i}(t) & \left|\angle\nabla_{x_j,x_i}(t)\right| < \left|\angle\nabla_{x_i,x_j}(t)\right| \end{cases}$$

This will cause the angle to be limited to +45 and −45 degrees and invariant to the choice of horizontal or vertical axis. In addition, as the phase will be undefined if $x_i(t) = x_i(t-1)$, in this case $\angle\nabla_{x_i,x_j}(t)$ will be equal to zero. The same statement holds when $x_j(t) = x_j(t-1)$.

We believe $\angle\nabla_{x_i,x_j}(t)$ can act as a measure for functional connectivity (i.e. covariance between x_i and x_j). If the two time series are highly correlated (time series i vary very similarly to time series j), the gradient of these two time series would tend to form 45 degree with the i axis. $\angle\nabla_{x_i,x_j}(t)$ will be referred to as instantaneous shared trajectory (IST) for the remainder of this manuscript.

To demonstrate the relationship between the covariance matrix and the pair of $\angle\nabla_{x_1,x_2}(t)$ and $|\nabla_{x_1,x_2}(t)|$, two time series were simulated using multivariate Gaussian probability density function (pdf):

$$[x_1(t), x_2(t)] \sim N\left(0, \begin{bmatrix} {\sigma_{1,1}}^2 & \rho\,\sigma_{1,1}\sigma_{2,2} \\ \rho\,\sigma_{1,1}\sigma_{2,2} & {\sigma_{2,2}}^2 \end{bmatrix}\right)$$

Values for $\sigma_{1,1}$ and $\sigma_{2,2}$ were between 0.1 and 1. The correlation ρ had values with a range between −1 and 1. For each possible value of these three parameters, the 2 time series were generated with length equal to 300 time points. Next their angle (i.e. IST) and magnitude values were calculated for every time points. These values were then averaged, i.e. for each generated time series pair, we have one value (averaged) for IST and one for magnitude of the gradient. This simulation was repeated 1000 times.

Figure 2 illustrates these values where the x axis is one of our variable parameters while the y axis in the first and second rows are average IST and average magnitude, respectively. As can be seen in Figure 2, the average IST does not change with the variance of the two time series while it clearly changes with ρ (this does not mean that IST is independent of the variance). In contrast, the average magnitude values change primarily as a function of $\sigma_{1,1}$ and $\sigma_{2,2}$ while remaining mostly constant with respect to ρ. One interesting insight here is that while the average IST does not change with $\sigma_{1,1}$ and $\sigma_{2,2}$, its standard deviation does change. This suggests that the estimator (namely angle of the gradient) standard deviation increases as variance values of the original time series increase. This is quite similar to the presence of standard deviation in standard error formula of some of the most well-known estimators like sample mean (Ahn & Fessler, 2003; Bondy & Zlot, 1976).

To obtain an improved estimation of connectivity, we define a new estimator called weighted average of shared trajectory (WAST) by calculating the weighted average IST over a range of t−w and t+w:

$$WAST_{i,j}(t) = \frac{\sum_{k=t-w}^{t+w} \angle\nabla x_i, x_j(k) \times \left|\nabla x_i, x_j(k)\right|}{\sum_{k=t-w}^{t+w} \left|\nabla x_i, x_j(k)\right|}$$

As can be seen in the formula above, we are calculating the average of $\angle\nabla_{x1,x2}(k)$ using $|\nabla_{x1,x2}(k)|$ as weights. As we showed in Figure 2, $|\nabla_{x1,x2}(k)|$ can act as a metric for the variance of the two time series. To make the units comparable to the SWPC values, all the reported values for WAST in this paper are divided by the value 45 (as the values of SWPC are between −1 and +1 while IST values are between +45 and −45).

Multiplication of temporal derivatives (MTD)

As mentioned in the introduction section, Shine et al., proposed MTD as an alternative approach to SWPC to estimate connectivity (Shine et al., 2015). The MTD approach, shares some resemblance with WAST and both methods aim to estimate connectivity using a smaller number of samples (in contrast to SWPC method where a larger number of samples are required to reach a robust estimation). Therefore, we have done some comparison between MTD and WAST in the current work.

The MTD formula is as follows:

$$MTD_{i,j}(t) = \frac{[x_i(t) - x_i(t-1)][x_j(t) - x_j(t-1)]}{\sigma_i \sigma_j}$$

Where σ_i is standard deviation of x_i (for the whole time series). Figure 2 (the third row) shows the relationship between average MTD values and the covariance matrix defined in the previous section. As can be seen in the figure, MTD essentially only estimates the covariance and does not estimate the variance. Shine et al, proposed using a simple moving average (SMA) with MTD:

$$SMA_{i,j}(t) = \frac{1}{2w+1} \sum_{t-w}^{t+w} MTD_{i,j}(t)$$

For the rest of this manuscript, MTD refers to its SMA variant (i.e. the averaged version of MTD).

Simulations:

In this section, we describe a series of simulations designed to study the proposed approach. In all simulations, time series were simulated using a multivariate Gaussian pdf (with mean 0).

One challenging aspect of studying dFNC is summarizing the estimated connectivity values. An approach that has been suggested for this purpose employs k-means clustering to find co-occurring connectivity patterns from the estimated dFNC values. This method has been applied successfully to methods like SWPC (E. Allen et al., 2014) and wavelet coherence (Yaesoubi, Allen, Miller, & Calhoun, 2015) to summarize connectivity related information. The benefit of this approach is that it provides an intuitive summary of several patterns of connectivity that tend to recur over time. We have designed all our simulations assuming that there are several underlying connectivity patterns driving the data generation. All the methods are evaluated in terms of their ability to estimate these connectivity patterns.

Simulation 1: For the first simulation, two time series (T = 300) with varying values of $\sigma_{1,2}$ (between −1 and +1) were simulated:

$$[x_1(t), x_2(t)] \sim \mathrm{N}\left(0, \begin{bmatrix} 1 & \sigma_{1,2} \\ \sigma_{1,2} & 1 \end{bmatrix}\right)$$

The aim of this simulation was to evaluate the relationship of the calculated WAST values with different correlation values (i.e., $\sigma_{1,2}$).

Simulation 2: For this simulation, our aim was to explore how much error is introduced when the true correlation is static (constant over time) but analysis assumes that the connectivity is time-varying. As such, we simulated two time series (T = 1000) with random (static) correlation between −1 and 1. For each simulated time series, we then calculated WAST and SWPC using different window sizes. We also calculated the static value of these two metrics, i.e. window size for each metric was calculated to cover the whole time series. The error was then defined as the mean squared error between the estimator (WAST and SWPC) values and their static values. This simulation was repeated 1000 times.

Simulation 3: Next, two time series with 0 mean and covariance −0.5, 0, and 0.5 were simulated (the covariance remained the same for the whole time series). The length of the time series was chosen to be 1000. We then analyzed the time series using both SWPC and WAST with different window sizes. This simulation was repeated 1000 times and the histograms of all the values (across all simulations) were calculated.

Simulation 4: The aim of our fourth simulation was to examine the performance of WAST, SWPC and MTD in different scenarios. To do this, nine time series were generated using a multivariate Gaussian pdf. The covariance matrix remained constant for a period of time (we call this period one state, and the length of each state is called dwell time), then changed to another value (another state). For this simulation, three states with different lengths were simulated. We performed multiple simulations using different state lengths (L_i) to explore different possible scenarios.

$$X \sim \mathrm{N}(0, \Sigma_t)$$

$$\Sigma_t \in \Sigma_i \qquad i = 1, 2, 3$$

For each Σ_t, we first randomly chose a variance value between 0 and 1 for all nine time series. Then based on the variance values we calculated the covariance entries (off-diagonal entries) between the connected time series pairs to have a correlation of 0.7. The covariance entries between the time series that were not connected were assigned a value of 0.

To compare the approaches, we used them to estimate the correlation matrix at each window using different window sizes. This step resulted in a 9×9 symmetric matrix so 9×8/2=36 values for each window. These were used as the input to a k-means clustering step (where 36 was number of features) to estimate 3 clusters (cluster centroid; C_i). These cluster centroids are essentially an estimate for the original Σ_i. To check the accuracy of these estimates, we defined two metrics.

- **Performance metric:** We calculated the similarity between cluster centroids (C_i) and the true correlation matrices (Σ_i; true correlation matrix used for simulation) using Pearson correlation as the distance metric. This resulted in 3 values for each C_i. Each value indicates how close C_i is to a given (Σ_i) in terms of the variations between their elements. We then count the values higher than 0.8 for each C_i (i.e. if a C_i and Σ_i pair have correlation higher than 0.8 we assume the estimation of Σ_i is accurate). Thus, for each cluster we have 0 to 3 as possible values. The most desirable value is 1 (in which case C_i is close to one and only one of the Σ_is), while the worst case is 0 (where C_i is not close to any of the Σ_i values). The other 2 values (2 and 3) mean that Σ_i is similar to more than one C_i. This allows us to include Σ_i in the final results (compared to the instance that the performance metric is zero where Σ_i information is lost completely). The ratio of 1s is then calculated as our performance metric. The reason we avoided using a measure like mean squared error to evaluate performance of the estimators is because calculating the mean squared error when the estimand varies by time is not straightforward. More importantly, our focus is on estimating the co-occurring connectivity patterns (i.e. states correlation matrices) rather than the actual dFNC values in the current work.
- **False positive metric:** To quantify the degree to which each method overestimates the null covariance, we first found respective states for each window (for both WAST and SWPC methods), and then using their Σ_i, we generated a mask to only include zero values of Σ_i (The true covariance matrix of each state):

$$M_i(a,b) = \begin{cases} 1 & \sum_i(a,b) = 0 \\ 0 & \sum_i(a,b) \neq 0 \end{cases}$$

Where a and b are correlation matrix indices.

This mask was then multiplied into each estimated value of WAST or SWPC, and the average of non-zero values was calculated. In other words:

$$fp_i = \frac{1}{N_i}\sum C_i(a,b) \quad \forall a,b \mid M_i(a,b) = 1$$
$$N_i = number\ of\ non\ zero\ elements\ of\ M_i$$

f_{p_i} values measure the amount of overestimation of zero correlation for each estimated state (i.e. C_i). The overall mean of f_{p_i} is then calculated for each simulation:

$$fp = \frac{1}{3}\sum_{i=1}^{3} fp_i$$

In this simulation, 3 scenarios are designed. In the first scenario, the dwell times of all the states are chosen to be very short. In the second scenario, the 3 states have different dwell times (one short, one medium length and one with large dwell time). For the third scenario, all the 3 states are chosen to be relatively large. Please note that the first scenario is designed to favor WAST /MTD while the third one is designed to favor SWPC.

Real data analysis:

The utilization of our proposed metric is demonstrated by analyzing a resting state fMRI dataset obtained as a part of the Functional Imaging Biomedical Informatics Research Network (fBIRN) project (Potkin & Ford, 2009). This dataset includes 163 healthy control (HC) and 151 schizophrenia patients (SZ). 162 volumes of echo planar imaging bold data were acquired using 3T scanners. The TR for all scans was 2 sec. Further details regarding acquisition parameters and data information be found in our earlier work (Damaraju et al., 2014). Preprocessing included motion correction, slice-timing correction, and despiking. The data was then registered to a common Montreal Neurological institute (MNI) template and resampled to 3 mm^3 isotropic voxels. Next The data was spatially smoothed using a Gaussian kernel with a 6 mm full width at halfmaximum (FWHM = 6 mm), and each voxel time course was variance normalized.

The data was then decomposed into 100 spatially independent time series and their associated spatial map using group independent component analysis (GICA). This method is implemented in the GIFT (http://trendscenter.org/software/gift) software (Calhoun, Adali, Pearlson, & Pekar, 2001; Erhardt et al., 2011). For the analysis, each subject's 162 time points were first reduced into 100 dimensions using principal component analysis (PCA). Next, all subject's data were concatenated and another PCA was used to reduce the dimension to 100. Finally, 100 maximally independent components were obtained from this data using ICA. We then visually inspected all 100 components and chose 47 components as intrinsic connectivity networks (ICNs). The ICN time courses were then band pass filtered between 0.01 and 0.15 Hz using a 5^{th} order Butterworth filter. For a full description of the analysis on the data please check (Damaraju et al., 2014).

The time series associated with these ICNs were used to calculate WAST and SWPC with different window sizes. The resulted values were clustered into 5 clusters. The cluster number was determined using elbow criteria (Thorndike, 1953). Next, the dwell time for each state was calculated for each subject. The dwell time is defined as the length of time each subject stay in one specific state after entering that state. The average mean dwell time is computed and compared between HC and SZ subjects.

Due to limitations imposed by the IRB of the original study we are unable to share the raw data, but it is possible to share the derived results, matrices and such upon direct request. In addition, all the code used in this study will be shared online and published as a part of the dFNC toolbox within GIFT (http://trendscenter.org/software/gift).

Results

Simulation Results:

First simulation—For the first simulation, two time series with correlation values between −1 and +1 were generated and static WAST (window size equal to the time series length) was calculated for each case. Figure 3 shows the non-linear mapping of correlation space resulted from WAST. As can be seen here the range of WAST is the same as the range of correlation but it has a slight non-linear tendency.

Second simulation: For the next simulation, two time series with random but constant covariance were generated and WAST and SWPC were calculated using different window sizes. These values were then subtracted from static WAST and Pearson correlation (i.e. window size equal to time series length) values to calculate error for each window size. The mean squared of these errors were reported. In addition, using the values computed and shown in Figure 3, we calculated a mapping of the SWPC values into WAST space and calculated the mean squared error based on these new values. The reason for this was to make sure the nonlinear nature of WAST does not impact the results greatly. Figure 4 illustrates the mean squared error (MSE) for different window sizes for all 3 methods. As seen here, the MSE for WAST is smaller than the other two for all window sizes. The MSE decreases for all methods as the size of window increases.

Third simulation: In the third simulation, the WAST and SWPC values for 2 time series with constant covariance of −0.5, 0 and +0.5 was calculated. The histogram of all the values for each covariance is shown in Figure 5. It is important to note that, as expected SWPC values for very small window sizes (e.g. 3) are heavily skewed toward the extreme values (+1 and −1), while WAST has resulted in the desirable normal-like histogram even for our smallest window size. The skewness of the SWPC values for small window sizes is caused by this estimator's high standard error for small sample numbers.

Fourth simulation:

Fourth simulation, Scenario 1: For the first scenario, all the states had very short dwell times (between 5 and 6 time points). Figure 6 show the performance metric for this simulation while Figure 7 shows the false positive values. As seen in Figure 6, using window

size 3 and 5, WAST has achieved an improved performance compared to both SWPC and MTD. SWPC combined with window size 3 has almost 0 as performance metric while MTD with the same window size has higher performance (above 0.75) but it has a very high standard deviation too (compared to WAST). All three methods have low performance values when paired with window sizes 10 and 20. This is likely because when using window sizes higher than 10 the short states are smoothed out (window size 10 is almost 2 times the true dwell time of all states). Please note that MTD has higher performance values compared to WAST and SWPC using window sizes 10 and 20 time point but its average value is lower compared to WAST paired with smaller window sizes and it has a very high standard deviation too. As seen in Figure 7, WAST shows less false positive values for almost all window sizes. As the false positive metric of both second and third scenarios were very similar to the first scenario, therefore we have only brought one figure (Figure 7).

Fourth simulation, scenario 2: In the second scenario, each state had different dwell time (5-6, 10-11, 15-16 time points) Figure 8 shows the performance metric for the second scenario. As seen in Figure 8, WAST has the highest average performance value for state 1 and 2 (window size 5) while for longer state (i.e. state 3) SWPC shows the same performance value compared to WAST. For almost all the states MTD has lower average (and higher standard deviation) compared to both WAST and SWPC. One exemption is that when paired with a window size equal to 5 time points, MTD has higher performance values compared to SWPC. Even in this situation WAST is showing higher performance for all states.

Please note that the performance of all methods for the shortest states is lower than what was reported for the first scenario (Figure 6). This is likely because of how the simulations are set up. When the dwell time of the states are different (as is the case in this scenario), the data spend less time in total in the shortest state compared to the longest state. This in turn, causes the k-means clustering to be biased toward longer states.

Fourth simulation, scenario 3: In the third scenario, all of the states had the same relatively large dwell time (20-21 time points). The performance values for the third scenario are depicted in Figure 9. For this scenario, WAST is showing very high (almost 1) performance values when paired with all window sizes while SWPC only shows high performance values when compared with window sizes larger than 3 time points. MTD shows overall lower average performance paired with higher standard deviation compared to WAST.

fBIRN resting fMRI results:

As mentioned in the method section, we calculated WAST and SWPC with different window sizes on the 47 ICNs extracted from fBIRN dataset. Figure 10 demonstrates the histogram of all the values calculated using WAST and SWPC with different window sizes (this histogram includes all the calculated values for both HC and SZ). As can be seen in Figure 10, the histogram of WAST values is similar to a Gaussian pdf even for very small window size (6s) while SWPC histogram for window sizes 6s and 10s are heavily skewed toward +1 and −1 values (related to spurious extreme values estimated due to the small sample size).

This is a well-known problem associated with the Pearson correlation. i.e. we need a large number of samples to obtain estimation with good standard error using Pearson correlation (Bowley, 1928).

The values of WAST and SWPC of each window size were then clustered using the k-means clustering approach. Figure 11 illustrates the cluster centroids for different window sizes when the cluster number is chosen as 5. The 5 clusters resulted from SWPC (except for the ones from SWPC with window size 6s) have been reported in our previous work too (Damaraju et al., 2014). Out of the 5 clusters identified from WAST, 4 of them are very similar to the ones from SWPC (clusters 1, 2, 4 and 5; See Figure 12 for the correlation between cluster centroids). However, cluster 3 from WAST looks quite different from those in SWPC. Interestingly the third cluster in SWPC with window size 6s is similar to this third cluster in WAST, but from Figure 10 we know that SWPC values from this window size (6s) are quite skewed toward +1 and −1.

Next, using the cluster index for all subjects, the mean dwell time was calculated for all states and a two-sample t-test was used to compare the mean dwell time between HC and SZ individuals. Figure 13 shows these results for different window sizes for both WAST and SWPC. Focusing on cluster 3 results, we see that in the case of SWPC results with smallest window size, the SZ subjects have higher mean dwell time (similar to the results from WAST for this specific cluster). For larger window sizes (i.e. 10s, 22s and 62s), both the cluster centroid (see Figure 11) and the direction of the effect changes, i.e., the mean dwell time for the HC subjects (compared to SZ) is higher for this cluster in larger window sizes. The direction of this result is quite similar to what we see for cluster 1 (for both WAST and SWPC). If we examine the cluster centroids in Figure 11, we can see that SWPC cluster 3 for the larger window sizes are quite similar to the cluster 1 centroids (see Figure 12). It has the same positive connectivity block between AUD, VIS and SM domains. The difference between SWPC cluster 3 and 1 (for window sizes 10s, 22s and 62s) is in the connectivities between DM domain and the three domains AUD, VIS and SM. These connectivities are mostly negative for cluster 1 while they are more positive for cluster 3.

Discussion

In this paper, we proposed a new estimator called WAST for dFNC based on the gradient of change and a sliding window. To compare WAST with SWPC (the most well-known estimator for dFNC) and MTD (another method designed to estimate dFNC in shorter time resolution), we designed different simulations and evaluation metrics. We found that WAST performed better in these designed simulations. We also utilized WAST on a real dataset including SZ and HC individuals and found similar results to the SWPC method in addition to findings that are exclusive to WAST.

We first showed how to calculate gradient of time series and used simulation to show that the angle of these gradients, changes with the covariance between the two time series while the magnitude changes with their variances. Our proposed estimator, WAST, uses the magnitude of gradients to calculate weighted average of angle for each window. The resulted values were then showed to non-linearly map correlation values. Next, we showed that

WAST has less error when the correlation is static (does not change with time) compared to SWPC. This difference was more visible in smaller window sizes. We also showed that, even when we use very short window sizes, WAST results in values with normal like histogram while SWPC values would be highly skewed to −1 and +1 when the window size is short. A histogram that is close to a Normal distribution is a desirable but not sufficient feature to show the benefits of WAST compared to SWPC. Both these observations point to the possibility that WAST has lower standard error compared to SWPC with the same sample size.

Next, we simulated a dataset with nine time series having three different connectivity states. We simulated different connectivity state lengths to compare the performance of WAST with SWPC and MTD. We were able to show that when the states are very short, by using small window sizes we can correctly estimate these states using WAST while if we use SWPC we are unable to estimate them. In addition, we showed that even if the states are long, WAST works at least as good as SWPC. It is important to note that in real data, we do not know the true length of states (how fast does connectivity change). As large window sizes are unable to detect short states, using shorter window size is desirable if the estimator is robust enough. However, using small window sizes causes high error for SWPC in comparison to WAST, which has high performance even for very small window sizes. We also showed that WAST results in lower false positive values compared to SWPC, when there is no connectivity in truth. In addition, in all three scenarios, we were able to show that WAST outperforms MTD (higher performance average paired with lower performance standard deviation).

The similarity between the formula for MTD and our method is that both of them include a derivative term for x_i and x_j. Please note that there is multiplication between the derivative terms in MTD while in WAST there is division between those terms (This is an important difference). As we showed in the methods section of this paper, WAST is based on the graphical representation of the time series pairs in their defined shared 2D space (Figure 1). In this 2D space angle and magnitude of the gradients are calculated. The reason for the presence of derivative terms in the formula for WAST is that we are estimating gradient using the first derivative. There are many ways to estimate the gradient, but we start with the most straightforward approach, i.e. using the first derivative. Please note that in the derivative formula we need to divide the results by the time difference between the two consecutive samples but as this is a constant number in our case, we decided to ignore that division as it will not impact the final results.

In the following sections, we discuss the fBIRN results.

Results shared between WAST and SWPC:

Here, we discuss the results that are the same between WAST and SWPC. These results have also been reported in our group's previous work where we utilized SWPC with window size 44s (Damaraju et al., 2014).

Based on the SWPC results (for window sizes 10s, 22s, and 62s), we can see that SZ subjects spend more time in cluster 5 which shows weak connectivities between different

domains in general (this cluster shows sparsely connected networks). We see a similar result for the WAST results as well. Apart from WAST window size 62s, SZ significantly spend more time in cluster 5 (which shows sparsely connected networks again). In addition, HCs stay longer in SWPC states 1 and 3 which show strong connectivities. Based on WAST results, we see the same effect direction for cluster 1. Please note that cluster 3 for WAST is quite different from cluster 3 of SWPC (see Figure 11). All these results can be used to infer that SZ show dysconnectivity between different networks. Dysconnectivity between different parts of the brain has long been hypothesized to be a possible cause for schizophrenia (Friston & Frith, 1995; He et al., 2013; Iraji, Deramus, et al., 2019; Iraji, Fu, et al., 2019; Miller et al., 2016; Stephan, Baldeweg, & Friston, 2006; Williamson & Allman, 2012). The presence of these connectivity patterns using all window sizes for the two approach, point to the slow nature of them in contrast with the connectivity pattern present in WAST cluster 3.

Results different between WAST and SWPC:

One connectivity pattern that is present in the WAST results but absent in the SWPC results is WAST cluster 3. This cluster shows negative connectivity between SM and the two sensory domains (i.e. AUD and VIS). Using wavelet decomposition Yaesoubi et al. found a similar coherence pattern when clustering only SZ (Yaesoubi et al., 2017). They were unable to find this specific pattern when clustering both HC and SZ together therefore no statement could be made about the significance of this state. In contrast to Yaesoubi et al. work, here we find a similar connectivity pattern (WAST cluster 3) using all the data. In addition, we show that SZ spend significantly more time in this state. There is considerable evidence supporting the presence of connectivity between motor areas and sensory regions for different cognitive tasks such as speech perception and production (D'Ausilio et al., 2009; Londei et al., 2010) in healthy individuals. In the past years, several studies have examined the sensorimotor connectivities in SZ compared to HC subjects. Kaufmann et al. reported a reduction in connectivity within sensorimotor nodes in SZ subjects (Kaufmann et al., 2015). In another study it was shown that connectivity in sensorimotor areas was lower in SZ compared to HC group (Berman et al., 2016). In contrast with the mentioned studies, we have not compared the connectivities in these regions between SZ and HC individuals and can only say that the SZ group spends more time in a state that shows negative connection between sensory (AUD and VIS) and motor (SM) domains. This alteration can be an explanation for hallucinations and delusions associated with schizophrenia.

A similar pattern is visible in SWPC cluster 3 using window size 6 sec. Using very small window size for SWPC has resulted in skewed values (see Figure 10), but because of using k-means clustering, we have been able to see the short pattern (negative connectivity between sensory and motor networks). This statement is supported by the fact that even in WAST results this short pattern is weakened and smoothed for larger window sizes.

Another (and not desirable) possible reason for the presence of this pattern in WAST cluster 3 can be the non-linear way WAST maps the correlation values (see Figure 2). To explore this possibility, we used the values calculated using SWPC (for all window sizes) and mapped those values using the previously calculated curve in Figure 3. Then, we applied k-

means clustering on these values (which have the same non-linearity as the WAST metric). The resulted clusters did not change significantly compared to SWPC results, and we were still unable to obtain WAST cluster 3. In addition, WAST results show 4 clusters that are quite similar to SWPC results, so the new cluster does not appear to be caused by the non-linear nature of WAST.

One additional advantage of our proposed metric (WAST) over SWPC is that by using derivative, WAST can possibly reduce the effect of auto-regression on the estimated connectivities. This is a well-known limitation of the SWPC which has been mentioned in other works (Afyouni, Smith, & Nichols, 2018; Arbabshirani et al., 2014). This claim needs further examination in future work and is outside the scope of this work.

Limitations:

One limitation of WAST is that it maps the correlation space non-linearly (see Figure 3). The reason we did not apply the transformation (Figure 3) to make WAST as linear as possible was to avoid making the method more complex. In addition, this non-linear effect is less important in our approach to dFNC analysis since the estimated dFNC values are not typically reported and interpreted by themselves. Instead, the estimated values are used to find co-occurring connectivity patterns, where the relative values between different parts of the brain are important.

Another limitation of this paper is that the simulation is not mirroring more fMRI-like properties. For example, our designed simulations do not include autocorrelation effects (a known property of the fMRI signal). The reason we decided to design our simulations without any autocorrelation is because we view WAST as a general method for estimating dynamic correlation/co-occurrence on any dataset (possibly without any inherent autocorrelation). Therefore, our aim was to showcase WAST in a more general setting in this initial work. In addition, using WAST on real data we managed to estimate 4 states that are quite similar to SWPC results, with an additional (possibly higher frequency) state that we are able to capture more robustly than previous studies, suggesting the WAST approach works well on real fMRI data.

Finally, we do not compare WAST to approaches such as instantaneous phase coherence (Cabral, Kringelbach, & Deco, 2017) or window-less dictionary learning (Yaesoubi et al., 2018). We focus on a comparison of WAST with MTD for two key reasons. Firstly, we included MTD because the formulation is similar to that of WAST and thus is conducive to a more detailed comparison. Doing a detailed comparison with these and other methods is better addressed in a subsequent project. Secondly, we view WAST as a window-based approach and therefore comparing them with instantaneous connectivity estimation is not straightforward. Window based approaches (e.g. SWPC) use neighbor samples and therefore have lower standard error if connectivity is slower (in the most extreme case constant). Instantaneous connectivity estimators aim to estimate more rapid changes in connectivity (in the most extreme case connectivity is changing between each consecutive sample). One disadvantage of Instantaneous connectivity estimators is their higher standard error if the true connectivity is static or changing very slowly. Considering these two reasons in this work we chose to compare WAST with two window-based approach (i.e. SWPC and MTD)

and leave a more comprehensive comparison between different methods (both window-based and instantaneous) for future study.

Conclusion:

Results suggest that weighted average of shared trajectory (WAST) is a good alternative to SWPC for estimating dFNC, particularly because it allows us to use shorter window length and therefore improve our ability to detect brain states. In other words, WAST requires fewer samples to reach the same results which allow us to identify faster changes in dFNC with more reliability. Here we showed the superiority of WAST to SWPC and MTD using several simulation scenarios. We also utilized WAST for a multi-site fMRI dataset including HC and SZ individuals. In addition to some shared results between WAST and SWPC, we identified an interesting state which was undetected by the typical SWPC method. The estimated state showed negative connectivity between sensory and motor domains. Results also suggest that SZ individuals stay in this state longer compared to HC. Here, we speculate that this alteration (which is not visible using SWPC) may be linked to the hallucinations and delusions associated with schizophrenia, though future work will be needed to test this.

Acknowledgements

Data collection was supported by the National Center for Research Resources at the National Institutes of Health (grant numbers: NIH 1 U24 RR021992, NIH 1 U24 RR025736-01, R01EB020407, P20GM103472, P30GM122734) and the National Science Foundation (1539067).

References:

Afyouni S, Smith SM, & Nichols TE (2018). Effective Degrees of Freedom of the Pearson's Correlation Coefficient under Serial Correlation. *bioRxiv*, 453795. Retrieved from https://www.biorxiv.org/content/biorxiv/early/2018/10/25/453795.full.pdf. doi: 10.1101/453795

Ahn S, & Fessler JA (2003). Standard errors of mean, variance, and standard deviation estimators.

Allen E, Damaraju E, Plis S, Erhardt E, & … (2014). Tracking whole-brain connectivity dynamics in the resting state. Cerebral …. Retrieved from https://academic.oup.com/cercor/article-abstract/24/3/663/394348.

Allen EA, Damaraju E, Plis SM, Erhardt EB, Eichele T, & Calhoun VD (2014). Tracking whole-brain connectivity dynamics in the resting state. Cereb Cortex, 24(3), 663–676. Retrieved from https://www.ncbi.nlm.nih.gov/pubmed/23146964. doi:10.1093/cercor/bhs352 [PubMed: 23146964]

Arbabshirani MR, Damaraju E, Phlypo R, Plis S, Allen E, Ma S, … Calhoun VD (2014). Impact of autocorrelation on functional connectivity. Neuroimage, 102 Pt2, 294–308. Retrieved from https://www.ncbi.nlm.nih.gov/pubmed/25072392. doi:10.1016/j.neuroimage.2014.07.045 [PubMed: 25072392]

Berman RA, Gotts SJ, McAdams HM, Greenstein D, Lalonde F, Clasen L, … Rapoport J (2016). Disrupted sensorimotor and social-cognitive networks underlie symptoms in childhood-onset schizophrenia. Brain, 139(Pt 1), 276–291. Retrieved from https://www.ncbi.nlm.nih.gov/pubmed/26493637. doi:10.1093/brain/awv306 [PubMed: 26493637]

Bondy WH, & Zlot W (1976). The Standard Error of the Mean and the Difference between Means for Finite Populations. The American Statistician, 30(2), 96 Retrieved from http://www.jstor.org/stable/2683803. doi:10.2307/2683803

Bowley AL (1928). The standard deviation of the correlation coefficient. Journal of the American Statistical Association, 23(161), 31–34. Retrieved from <Go to ISI>://WOS:000188339000004. doi:Doi 10.2307/2277400

Cabral J, Kringelbach ML, & Deco G (2017). Functional connectivity dynamically evolves on multiple time-scales over a static structural connectome: Models and mechanisms. Neuroimage, 160, 84–96.

Retrieved from https://www.ncbi.nlm.nih.gov/pubmed/28343985. doi:10.1016/j.neuroimage.2017.03.045 [PubMed: 28343985]

Calhoun VD, Adali T, Pearlson GD, & Pekar JJ (2001). A method for making group inferences from functional MRI data using independent component analysis. Hum Brain Mapp, 14(3), 140–151. Retrieved from https://www.ncbi.nlm.nih.gov/pubmed/11559959. doi:doi:10.1002/hbm.1048 [PubMed: 11559959]

Chang C, & Glover GH (2010). Time-frequency dynamics of resting-state brain connectivity measured with fMRI. Neuroimage, 50(1), 81–98. Retrieved from https://www.ncbi.nlm.nih.gov/pubmed/20006716. doi:10.1016/j.neuroimage.2009.12.011 [PubMed: 20006716]

D'Ausilio A, Pulvermuller F, Salmas P, Bufalari I, Begliomini C, & Fadiga L (2009). The motor somatotopy of speech perception. Curr Biol, 19(5), 381–385. Retrieved from https://www.ncbi.nlm.nih.gov/pubmed/19217297. doi:10.1016/j.cub.2009.01.017 [PubMed: 19217297]

Damaraju E, Allen EA, Belger A, Ford JM, McEwen S, Mathalon DH, … Calhoun VD (2014). Dynamic functional connectivity analysis reveals transient states of dysconnectivity in schizophrenia. Neuroimage Clin, 5, 298–308. Retrieved from https://www.ncbi.nlm.nih.gov/pubmed/25161896. doi:10.1016/j.nicl.2014.07.003 [PubMed: 25161896]

Erhardt EB, Rachakonda S, Bedrick EJ, Allen EA, Adali T, & Calhoun VD (2011). Comparison of multi-subject ICA methods for analysis of fMRI data. Hum Brain Mapp, 32(12), 2075–2095. Retrieved from https://www.ncbi.nlm.nih.gov/pubmed/21162045. doi:10.1002/hbm.21170 [PubMed: 21162045]

Friston KJ, & Frith CD (1995). Schizophrenia: a disconnection syndrome? Clin Neurosci, 3(2), 89–97. Retrieved from https://www.ncbi.nlm.nih.gov/pubmed/7583624. [PubMed: 7583624]

Hare SM, Ford JM, Mathalon DH, Damaraju E, Bustillo J, Belger A, … Turner JA (2019). Salience-Default Mode Functional Network Connectivity Linked to Positive and Negative Symptoms of Schizophrenia. Schizophr Bull, 45(4), 892–901. Retrieved from https://www.ncbi.nlm.nih.gov/pubmed/30169884. doi:10.1093/schbul/sby112 [PubMed: 30169884]

He Z, Deng W, Li M, Chen Z, Jiang L, Wang Q, … Li T (2013). Aberrant intrinsic brain activity and cognitive deficit in first-episode treatment-naive patients with schizophrenia. Psychol Med, 43(4), 769–780. Retrieved from https://www.ncbi.nlm.nih.gov/pubmed/22883428. doi:10.1017/S0033291712001638 [PubMed: 22883428]

Hutchison RM, Womelsdorf T, Allen EA, Bandettini PA, Calhoun VD, Corbetta M, … Chang C (2013). Dynamic functional connectivity: promise, issues, and interpretations. Neuroimage, 80, 360–378. Retrieved from https://www.ncbi.nlm.nih.gov/pubmed/23707587. doi:10.1016/j.neuroimage.2013.05.079 [PubMed: 23707587]

Hutchison RM, Womelsdorf T, Gati JS, Everling S, & Menon RS (2013). Resting-state networks show dynamic functional connectivity in awake humans and anesthetized macaques. Hum Brain Mapp, 34(9), 2154–2177. Retrieved from https://www.ncbi.nlm.nih.gov/pubmed/22438275. doi:10.1002/hbm.22058 [PubMed: 22438275]

Iraji A, Deramus TP, Lewis N, Yaesoubi M, Stephen JM, Erhardt E, … Calhoun VD (2019). The spatial chronnectome reveals a dynamic interplay between functional segregation and integration. Hum Brain Mapp Retrieved from https://www.ncbi.nlm.nih.gov/pubmed/30884018. doi:10.1002/hbm.24580

Iraji A, Fu Z, Damaraju E, DeRamus TP, Lewis N, Bustillo JR, … Calhoun VD (2019). Spatial dynamics within and between brain functional domains: A hierarchical approach to study time-varying brain function. Hum Brain Mapp, 40(6), 1969–1986. Retrieved from https://www.ncbi.nlm.nih.gov/pubmed/30588687. doi:10.1002/hbm.24505 [PubMed: 30588687]

Kaufmann T, Skatun KC, Alnaes D, Doan NT, Duff EP, Tonnesen S, … Westlye LT (2015). Disintegration of Sensorimotor Brain Networks in Schizophrenia. Schizophr Bull, 41(6), 1326–1335. Retrieved from https://www.ncbi.nlm.nih.gov/pubmed/25943122. doi:10.1093/schbul/sbv060 [PubMed: 25943122]

Leonardi N, & Van De Ville D (2015). On spurious and real fluctuations of dynamic functional connectivity during rest. Neuroimage, 104, 430–436. Retrieved from https://www.ncbi.nlm.nih.gov/pubmed/25234118. doi:10.1016/j.neuroimage.2014.09.007 [PubMed: 25234118]

Liu X, & Duyn JH (2013). Time-varying functional network information extracted from brief instances of spontaneous brain activity. Proc Natl Acad Sci U S A, 110(11), 4392–4397. Retrieved from https://www.ncbi.nlm.nih.gov/pubmed/23440216. doi:10.1073/pnas.1216856110 [PubMed: 23440216]

Londei A, D'Ausilio A, Basso D, Sestieri C, Gratta CD, Romani GL, & Belardinelli MO (2010). Sensory-motor brain network connectivity for speech comprehension. Hum Brain Mapp, 31(4), 567–580. Retrieved from https://www.ncbi.nlm.nih.gov/pubmed/19780042. doi:10.1002/hbm.20888 [PubMed: 19780042]

Miller RL, Yaesoubi M, Turner JA, Mathalon D, Preda A, Pearlson G, … Calhoun VD (2016). Higher Dimensional Meta-State Analysis Reveals Reduced Resting fMRI Connectivity Dynamism in Schizophrenia Patients. PLOS ONE, 11(3), e0149849 Retrieved from https://www.ncbi.nlm.nih.gov/pubmed/26981625. doi:10.1371/journal.pone.0149849 [PubMed: 26981625]

Ou J, Xie L, Wang P, Li X, Zhu D, Jiang R, … Liu T (2013, 6-8 Nov. 2013). Modeling brain functional dynamics via hidden Markov models. Paper presented at the 2013 6th International IEEE/EMBS Conference on Neural Engineering (NER).

Potkin SG, & Ford JM (2009). Widespread cortical dysfunction in schizophrenia: the FBIRN imaging consortium. Schizophr Bull, 35(1), 15–18. Retrieved from https://www.ncbi.nlm.nih.gov/pubmed/19023124. doi:10.1093/schbul/sbn159 [PubMed: 19023124]

Shine JM, Koyejo O, Bell PT, Gorgolewski KJ, Gilat M, & Poldrack RA (2015). Estimation of dynamic functional connectivity using Multiplication of Temporal Derivatives. Neuroimage, 122, 399–407. Retrieved from https://www.ncbi.nlm.nih.gov/pubmed/26231247. doi:10.1016/j.neuroimage.2015.07.064 [PubMed: 26231247]

Stephan KE, Baldeweg T, & Friston KJ (2006). Synaptic plasticity and dysconnection in schizophrenia. Biol Psychiatry, 59(10), 929–939. Retrieved from https://www.ncbi.nlm.nih.gov/pubmed/16427028. doi:10.1016/j.biopsych.2005.10.005 [PubMed: 16427028]

Thorndike RL (1953). Who belongs in the family? Psychometrika, 18(4), 267–276. Retrieved from 10.1007/BF02289263. doi:10.1007/bf02289263

Williamson PC, & Allman JM (2012). A framework for interpreting functional networks in schizophrenia. Front Hum Neurosci, 6, 184 Retrieved from https://www.ncbi.nlm.nih.gov/pubmed/22737116. doi:10.3389/fnhum.2012.00184 [PubMed: 22737116]

Yaesoubi M, Adali T, & Calhoun VD (2018). A window-less approach for capturing time-varying connectivity in fMRI data reveals the presence of states with variable rates of change. Hum Brain Mapp, 39(4), 1626–1636. Retrieved from https://www.ncbi.nlm.nih.gov/pubmed/29315982. doi:10.1002/hbm.23939 [PubMed: 29315982]

Yaesoubi M, Allen EA, Miller RL, & Calhoun VD (2015). Dynamic coherence analysis of resting fMRI data to jointly capture state-based phase, frequency, and time-domain information. Neuroimage, 120, 133–142. Retrieved from https://www.ncbi.nlm.nih.gov/pubmed/26162552. doi:10.1016/j.neuroimage.2015.07.002 [PubMed: 26162552]

Yaesoubi M, Miller RL, Bustillo J, Lim KO, Vaidya J, & Calhoun VD (2017). A joint time-frequency analysis of resting-state functional connectivity reveals novel patterns of connectivity shared between or unique to schizophrenia patients and healthy controls. Neuroimage Clin, 15, 761–768. Retrieved from https://www.ncbi.nlm.nih.gov/pubmed/28706851. doi:10.1016/j.nicl.2017.06.023 [PubMed: 28706851]

Highlights:

- New estimator for dynamic connectivity can detect both rapid and slow changes.
- We found a new dynamic connectivity pattern prevalent in schizophrenia patients.
- The new pattern showed negative connectivity between motor and sensory regions.
- This pattern cannot be detected using sliding window Pearson correlation.

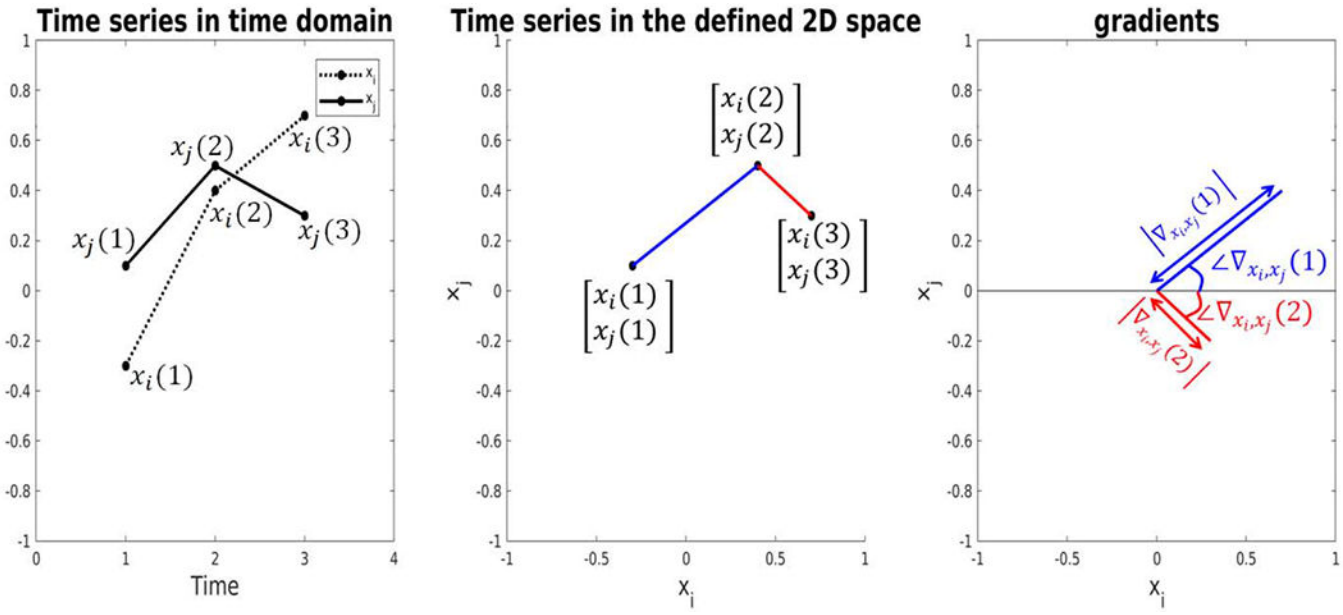

Figure 1.

This figure explains the main idea behind our proposed method. The left plot shows the two time series x_i and x_j in the time domain. The length of time series is 3 here. The middle plot shows the defined 2D space where x_i is horizontal and x_j is vertical axis. The colored vectors (blue and red) are the estimated gradients at time 1 and 2 respectively. The right plot shows the 2 gradient vectors in red and blue and what their angle and magnitude mean graphically. The angle here shows how much one time series varies in comparison to the other time series at each time point. For example, if the angle is close to zero, it means that x_j is not changing that much when x_i changes. In the other hand if the angle is close to 45 degree, it would mean x_j has changed very similarly to how x_i has changed.

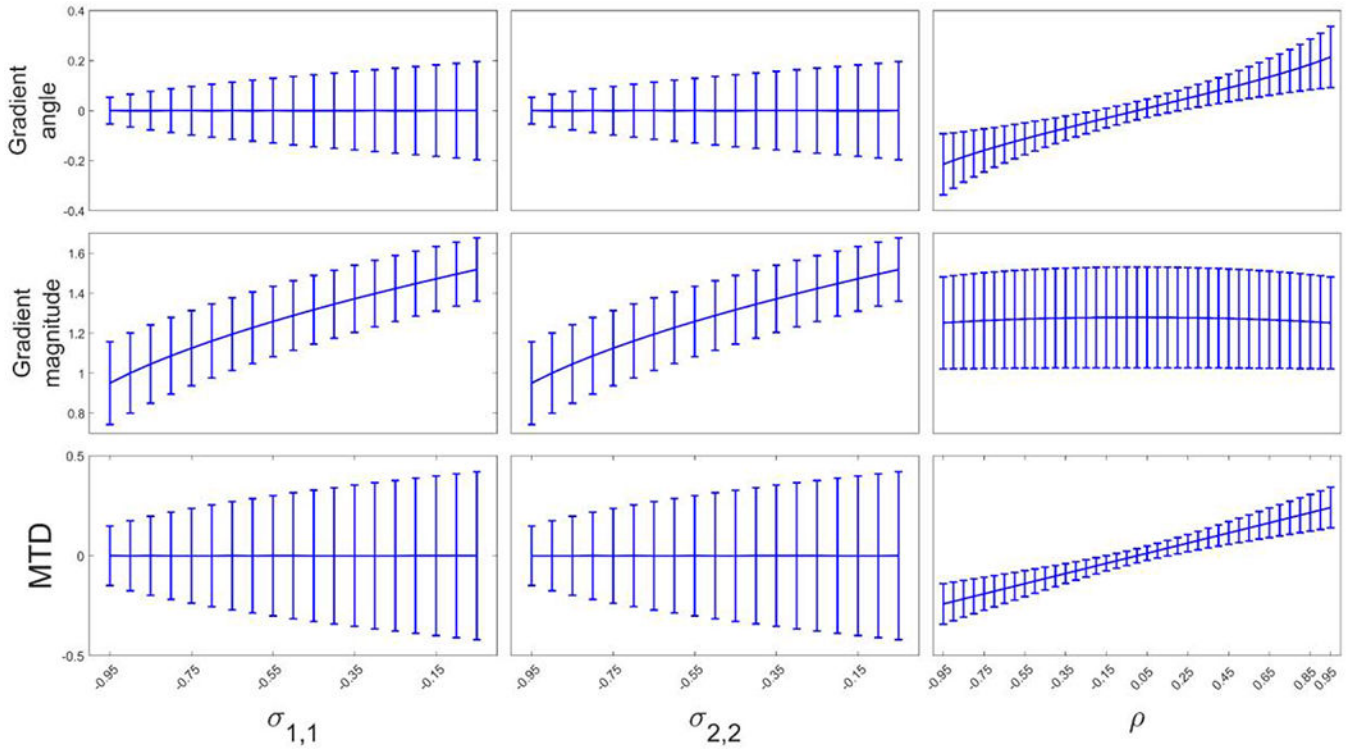

Figure 2.

The relationship between phase, gradient and MTD with the covariance matrix. As we can see here angle and MTD values change based on the ρ value (the top and bottom right figures). In contrast, the magnitude values change based on the variance of the two time series (middle two left figures). Based on this figure, we can say that WAST uses both covariance and variance information while MTD only uses covariance information and does not estimate variance.

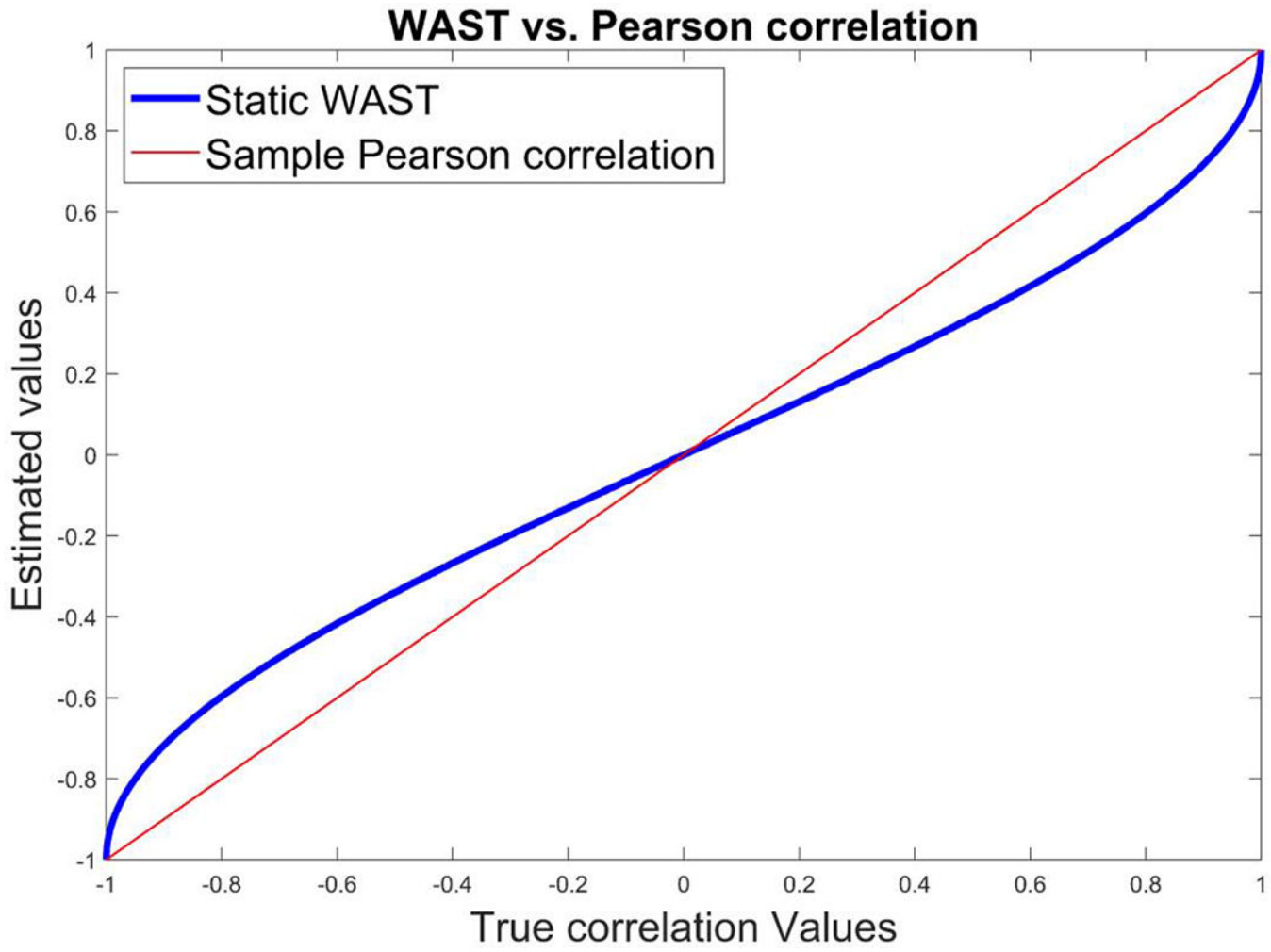

Figure 3.

The relationship between WAST and Pearson correlation values. WAST (the blue line) maps the covariance space in a non-linear fashion while the Pearson correlation (the red line) maps this space linearly. Based on this figure we can say that WAST is a biased estimator of connectivity while Pearson correlation is an unbiased estimator.

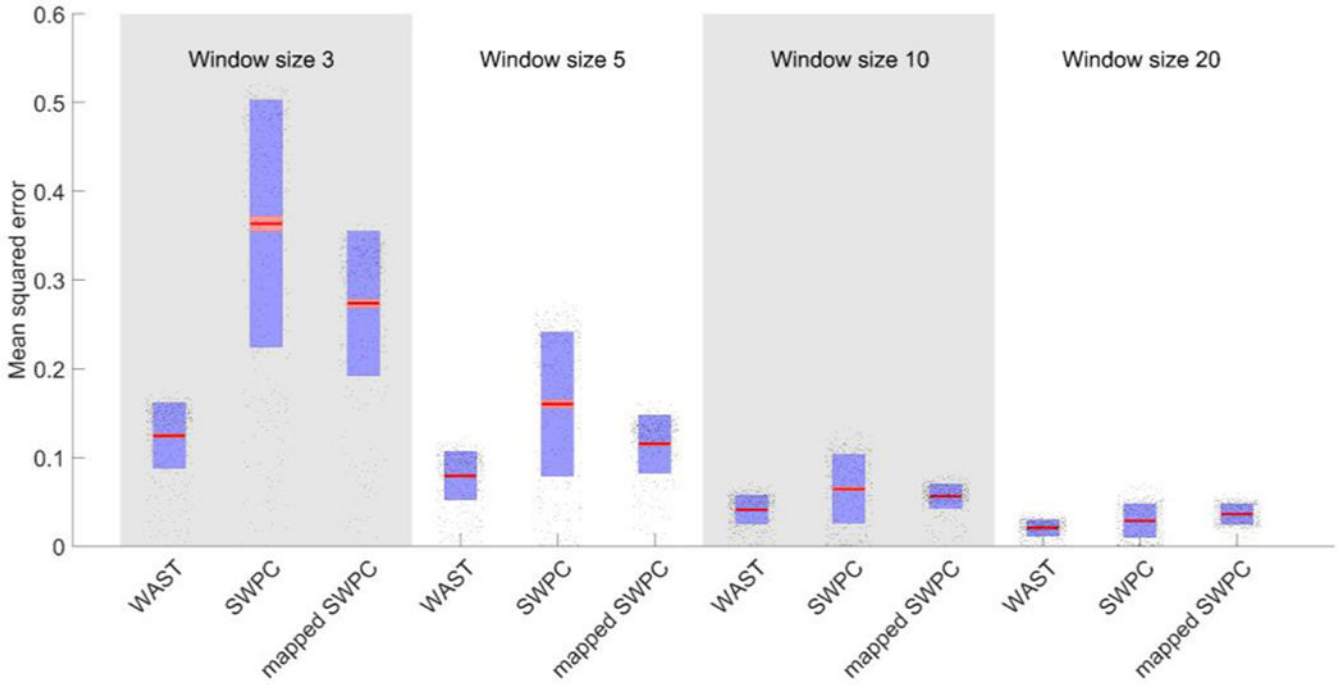

Figure 4.

Mean Squared error (MSE) of WAST and SWPC when the true covariance is static. To remove the non-linearity effect of WAST (see Figure 3), we transformed the SWPC using the values computed and shown in Figure 3 and brought the results here as well (called mapped SWPC). Based on these results WAST shows lower MSE compared to both SWPC and mapped SWPC for all window sizes. As expected, using larger window sizes decreases the bias of estimation and therefore the difference is smaller for larger window sizes.

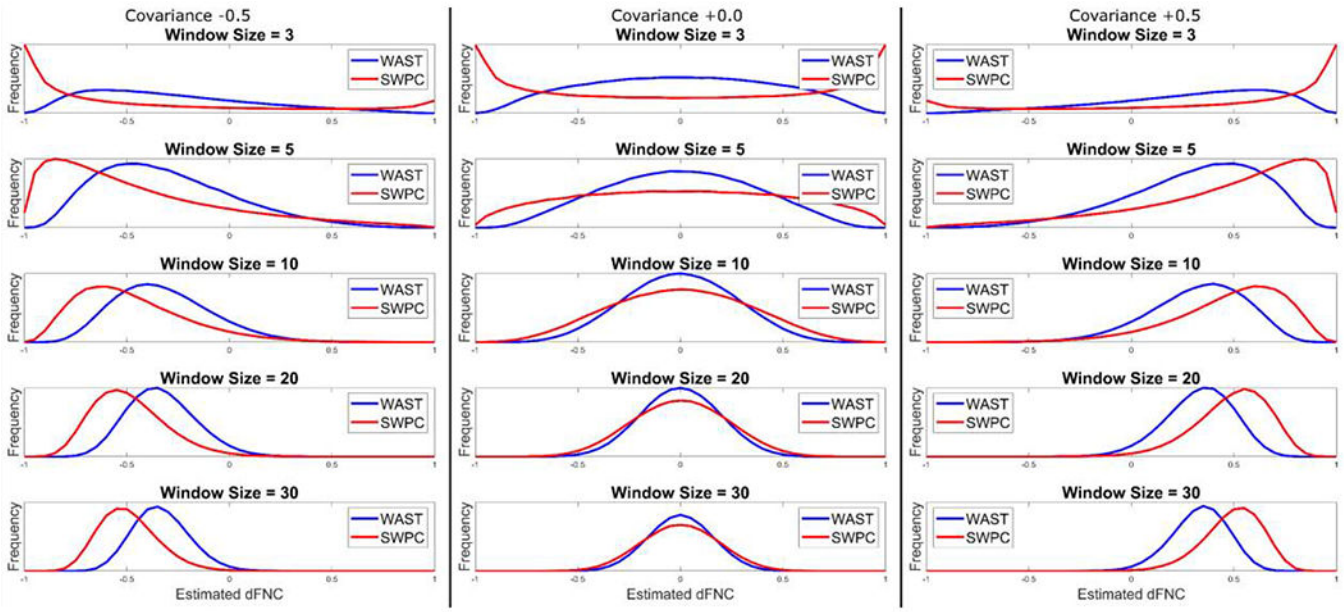

Figure 5.

The histogram of calculated values using WAST and SWPC with different window sizes. Here two time series with static covariance value (−0.5, 0, and +0.5) were simulated. Next WAST and SWPC were used to estimate covariance using different window sizes. As can be seen here WAST has normal like histogram even for small window sizes while SWPC values are skewed for small window sizes (window size 3 and 5). This suggests that WAST has lower standard error as an estimator for covariance compared to SWPC.

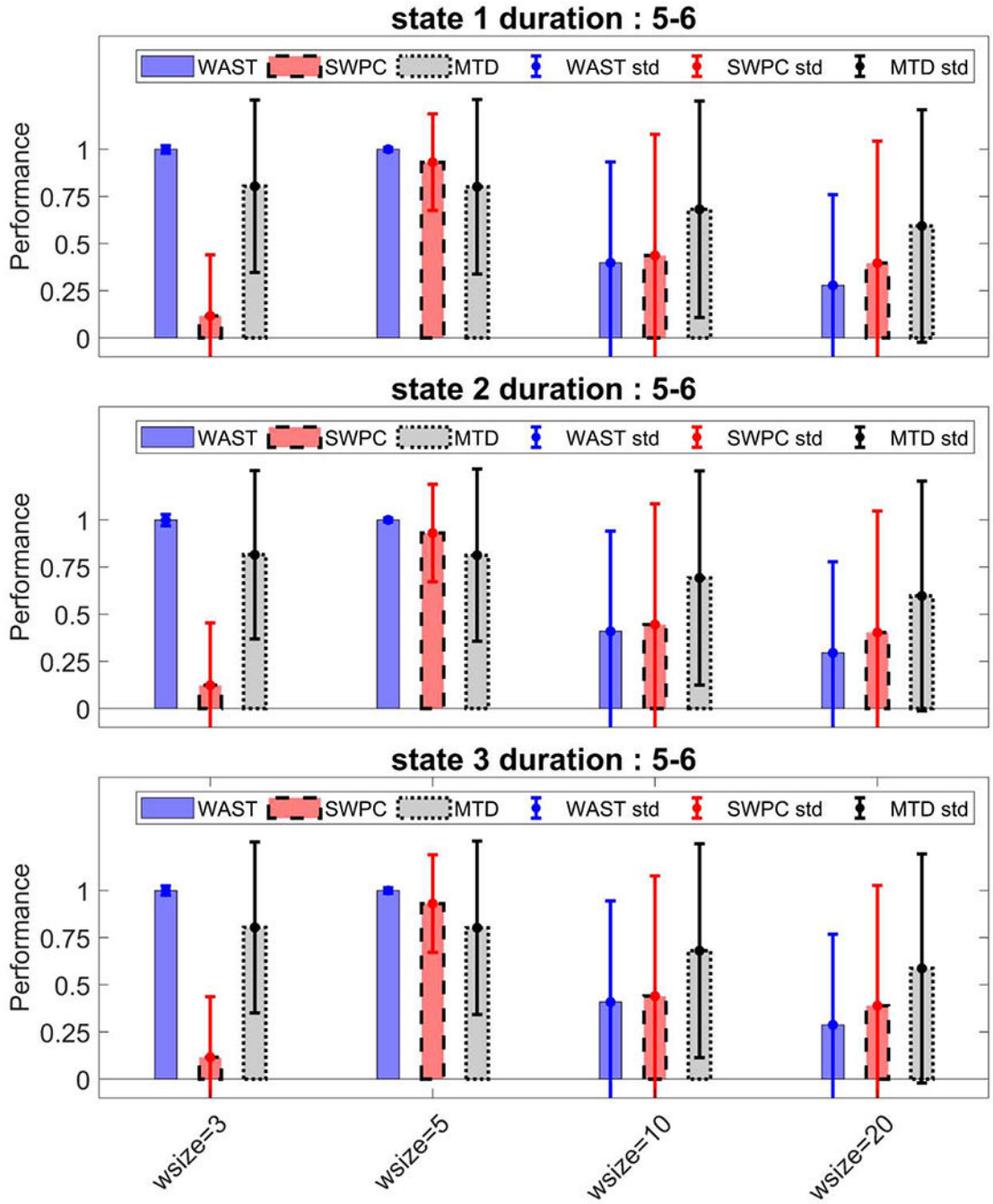

Figure 6.

Performance of the third simulation for the first scenario. Error bar represent the standard deviation of the performance metric for all the simulations. In this scenario, the state length was chosen to be small (between 5 and 6 time points). As seen here, WAST has been able to detect these states with higher performance compared to SWPC and MTD. For all three approaches, if we choose a window size more than 10 time points, the state is essentially undetected. In addition, note the higher error bar for both SWPC and MTD. This means that

WAST results are more robust (less varied between simulations) in addition to having overall higher mean (for window sizes 3 and 5 where performance is high).

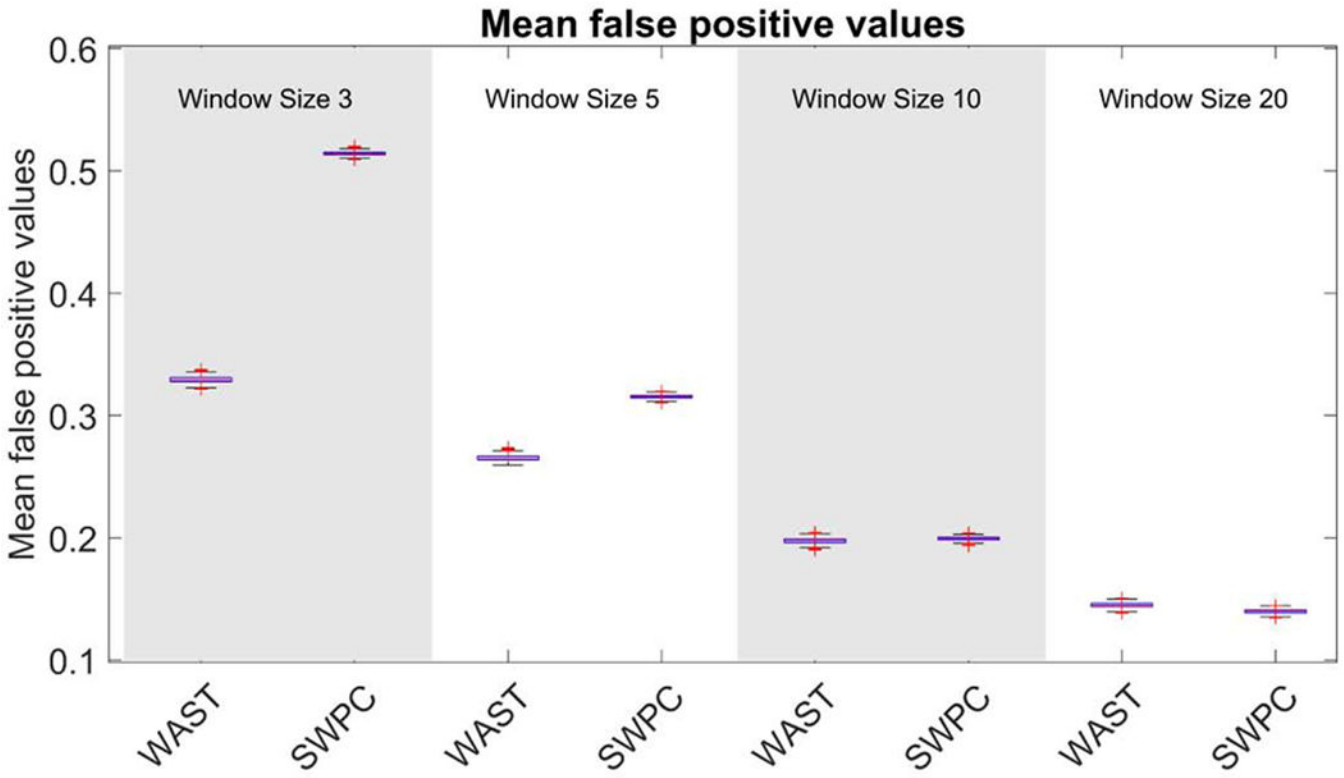

Figure 7.

Mean false positive for all of the scenarios in simulation 3. Here we have calculated how much each method falsely estimates null connectivities as a non-zero value. As seen here, WAST has lower mean false positive values (especially for small window sizes). As reported in Figure 4, this difference is smaller for larger window sizes, but using larger window sizes reduces the ability of both metrics to detect shorter states (See Figures 6 and 8).

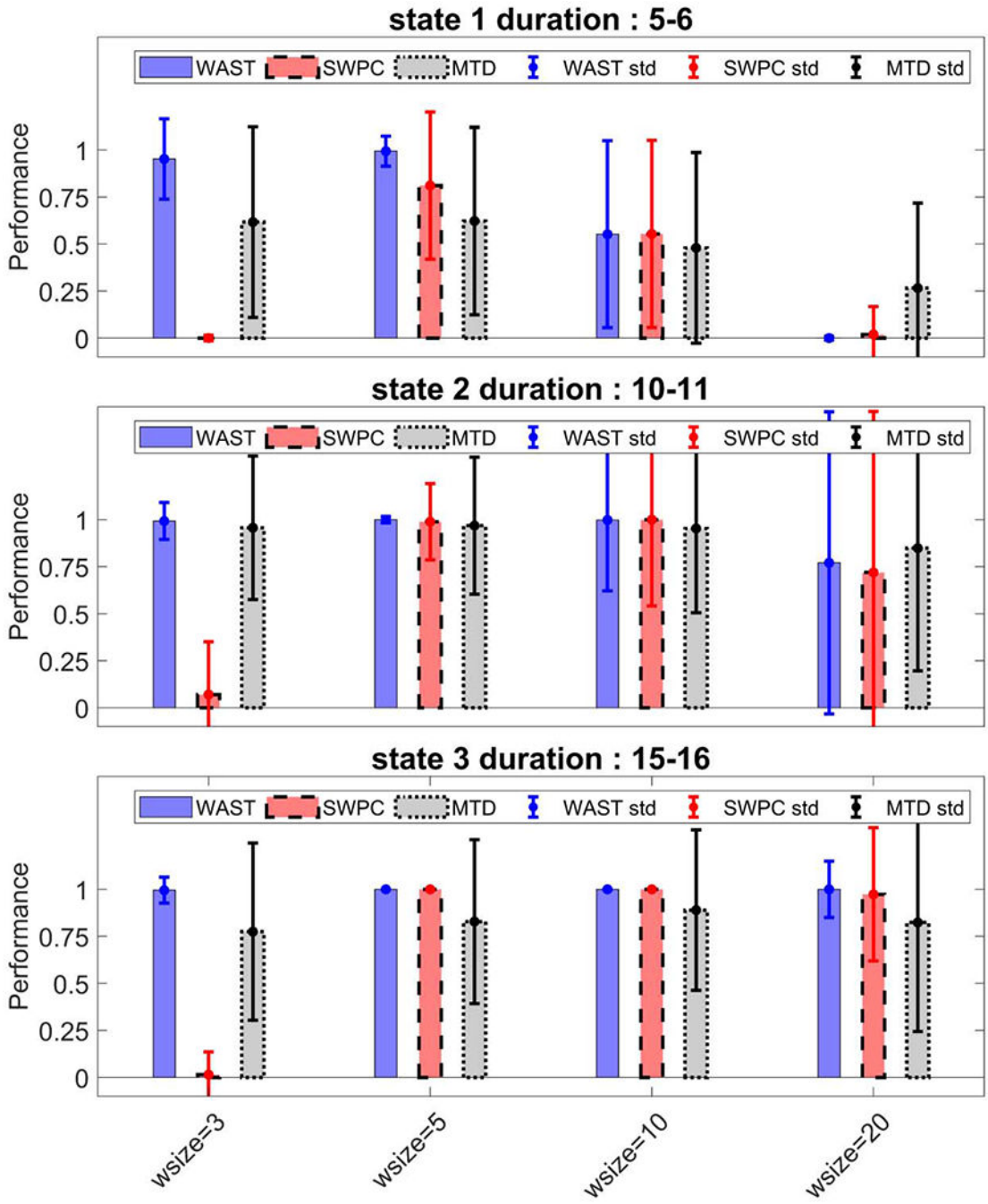

Figure 8.

Performance of the third simulation for the second scenario. Error bar represent the standard deviation of the performance metric for all the simulations. In this scenario, we had a very short state (with state length betWeen 5 and 6), and two longer states. For the very short state, as with the first scenario, WAST can detect this state more accurately compared to SWPC and MTD (as evidence by the higher value for performance). For the larger states, WAST has high performance even using window size 3 while to obtain good performance

values, SWPC needs at least a window size of 5. MTD shows lower average value paired with higher standard deviation.

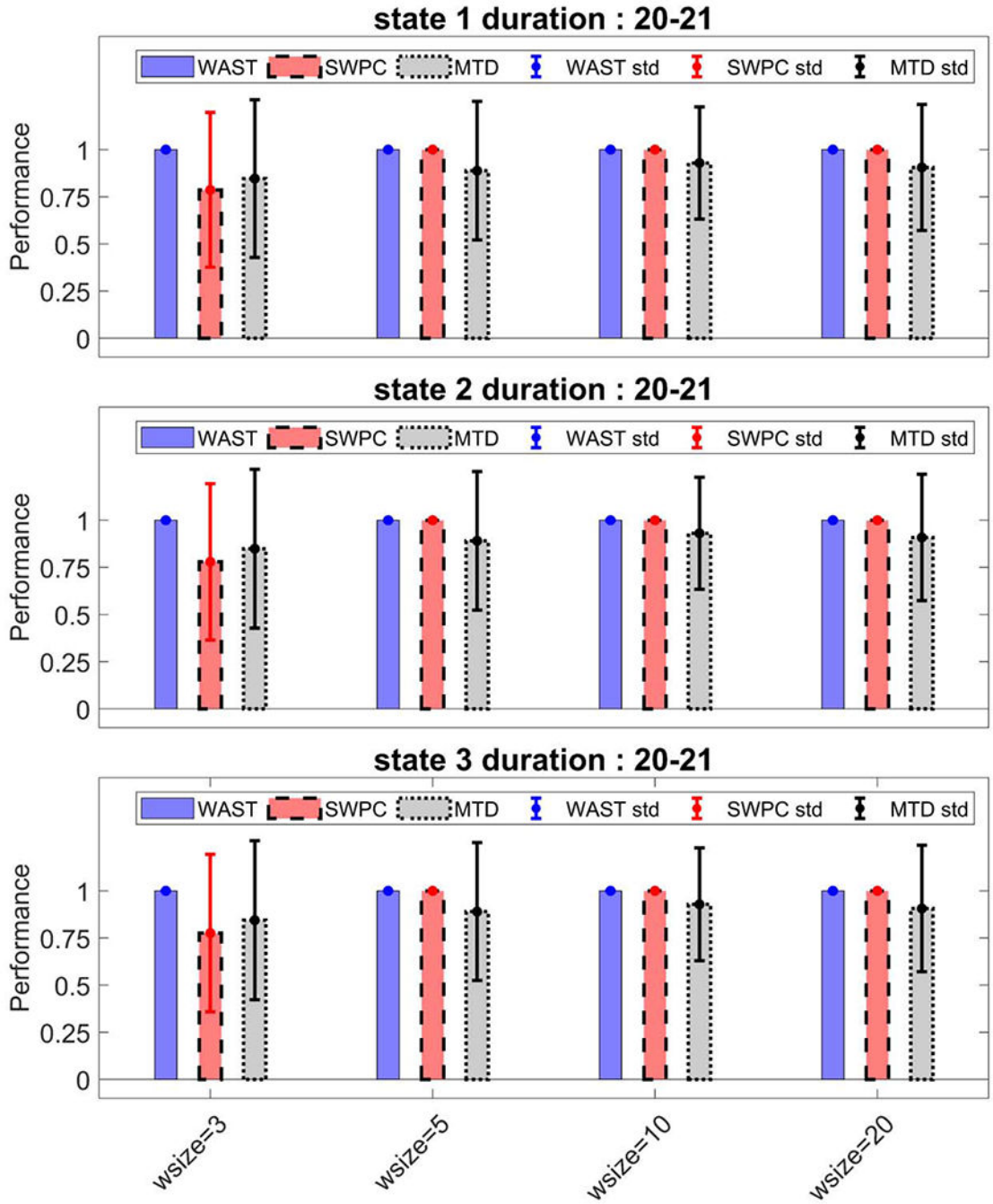

Figure 9.

Performance of the fourth simulation for the third scenario. Error bar represent the standard deviation of the performance metric for all the simulations. In this scenario, all the states had relatively long dwell times (between 20 and 21 time points). The results suggest that WAST has very high performance values with all the examined window sizes. In contrast, SWPC has high performance only for window sizes larger than 3 time points. This means that WAST can achieve high performance using a very small window size even when the actual

covariance is changing more slowly. In this scenario too, MTD shows lower average performance paired with higher standard deviation when compared with WAST.

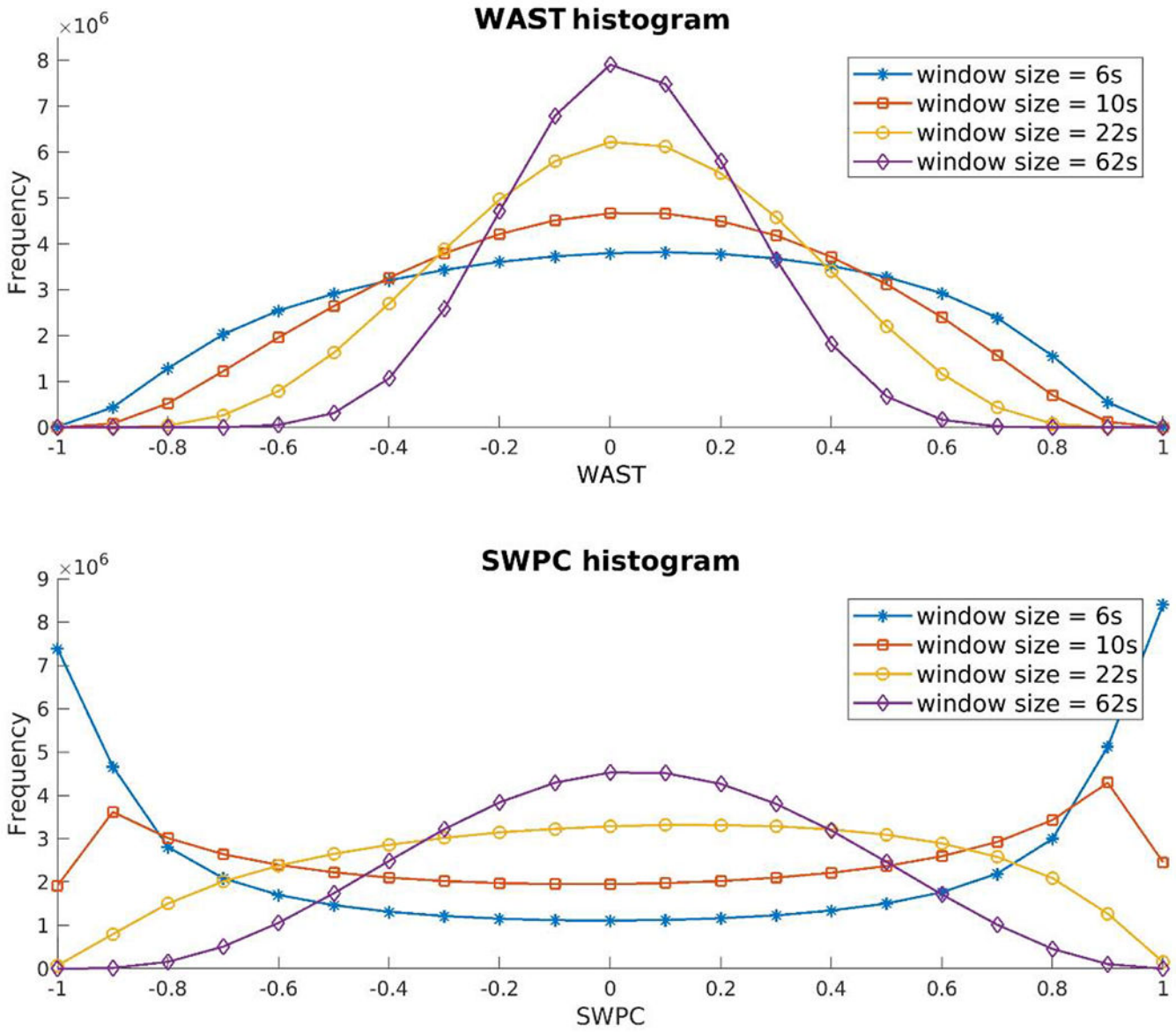

Figure 10.

The histogram of the calculated values from data using WAST and SWPC for different window sizes. As can be seen here, like what we saw in Figure 5 for simulated data, using small window sizes causes a skewness in calculated SWPC values. In contrast, even with very small window sizes, WAST is not skewed by spurious extreme values.

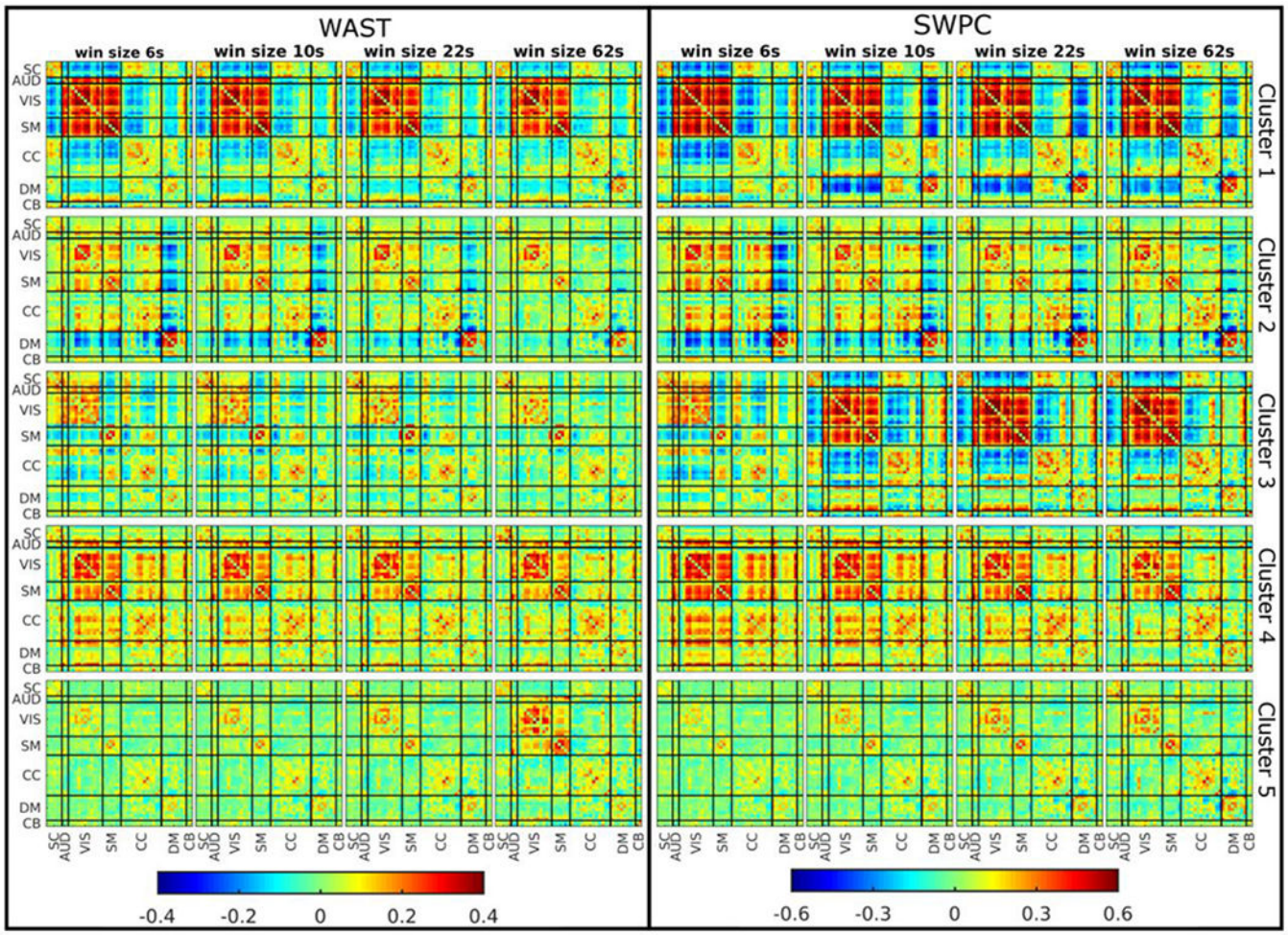

Figure 11.

k-means cluster centroids resulted from WAST and SWPC for several window sizes. 4 out of 5 clusters have very similar centroids between WAST and SWPC (i.e. clusters 1,2,4 and 5), while cluster 3 is visibly different. Cluster 3 in WAST shows strong connectivity between SC, AUD and VIS. In addition, the SM domain has negative connectivity with SC, AUD and VIS domains. This pattern is exclusive to WAST results (A similar pattern is estimated using window size 6s for SWPC). Note that cluster 3 in WAST results fades out for larger window sizes.

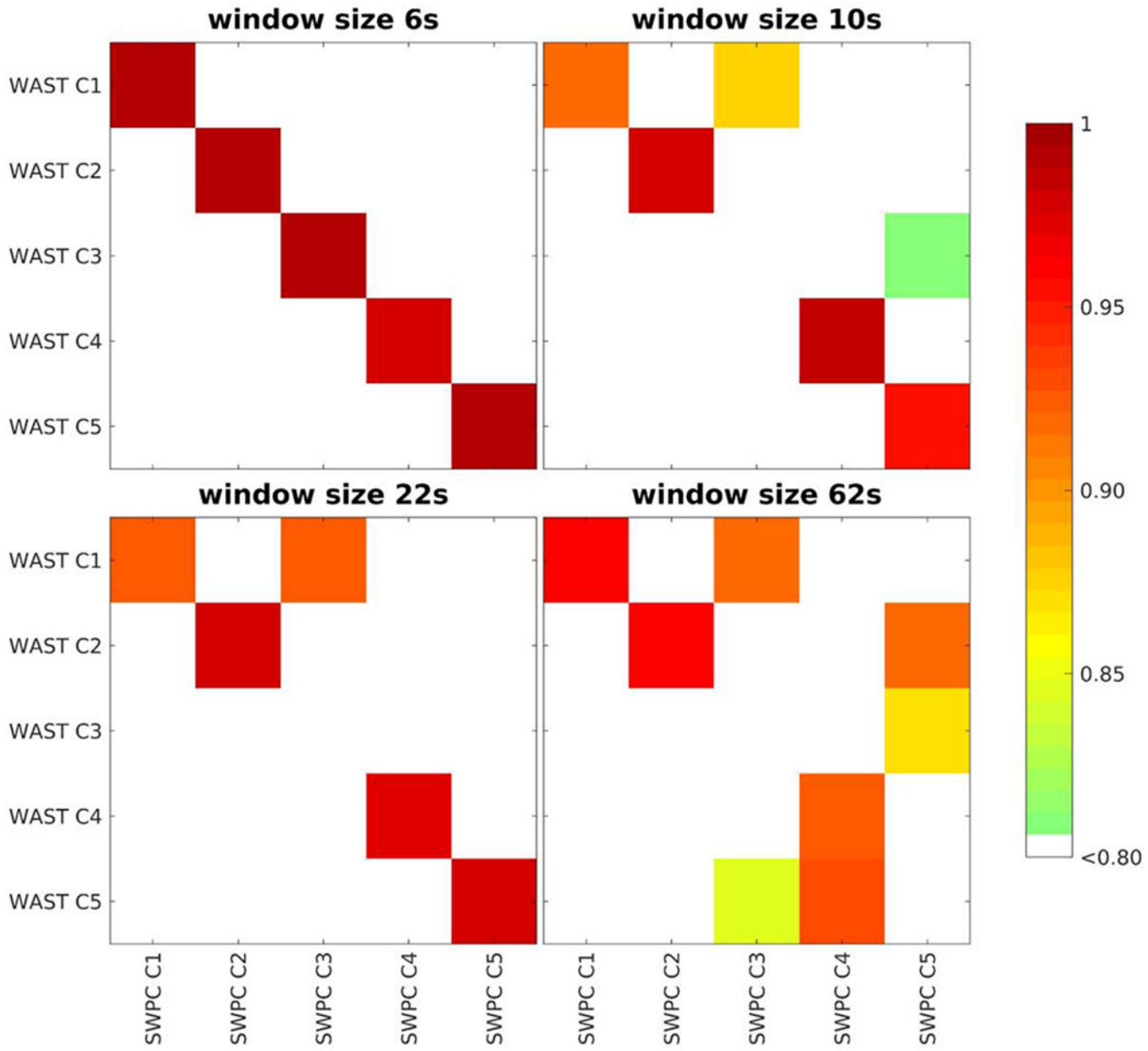

Figure 12.

Correlation between cluster centroids (shown in Figure 11). For the window size 6s, all 5 clusters from WAST are similar to the ones from SWPC (the correlation matrix has high values on the diagonal). For larger window sizes, cluster 3 for WAST diverges from cluster 3 of SWPC (It is similar to cluster 5 of SWPC but the correlation is below 0.9 here). In addition, as can be seen here, cluster 1 of WAST is similar to cluster 1 and 3 of SWPC for larger windows. As seen in Figure 11, cluster 1 and 3 of SWPC are similar to one another. In conclusion, it seems that there is less similarity between WAST clusters (as cluster 3 is quite different from cluster 1) compared to SWPC clusters (where cluster 1 and 3 are quite similar).

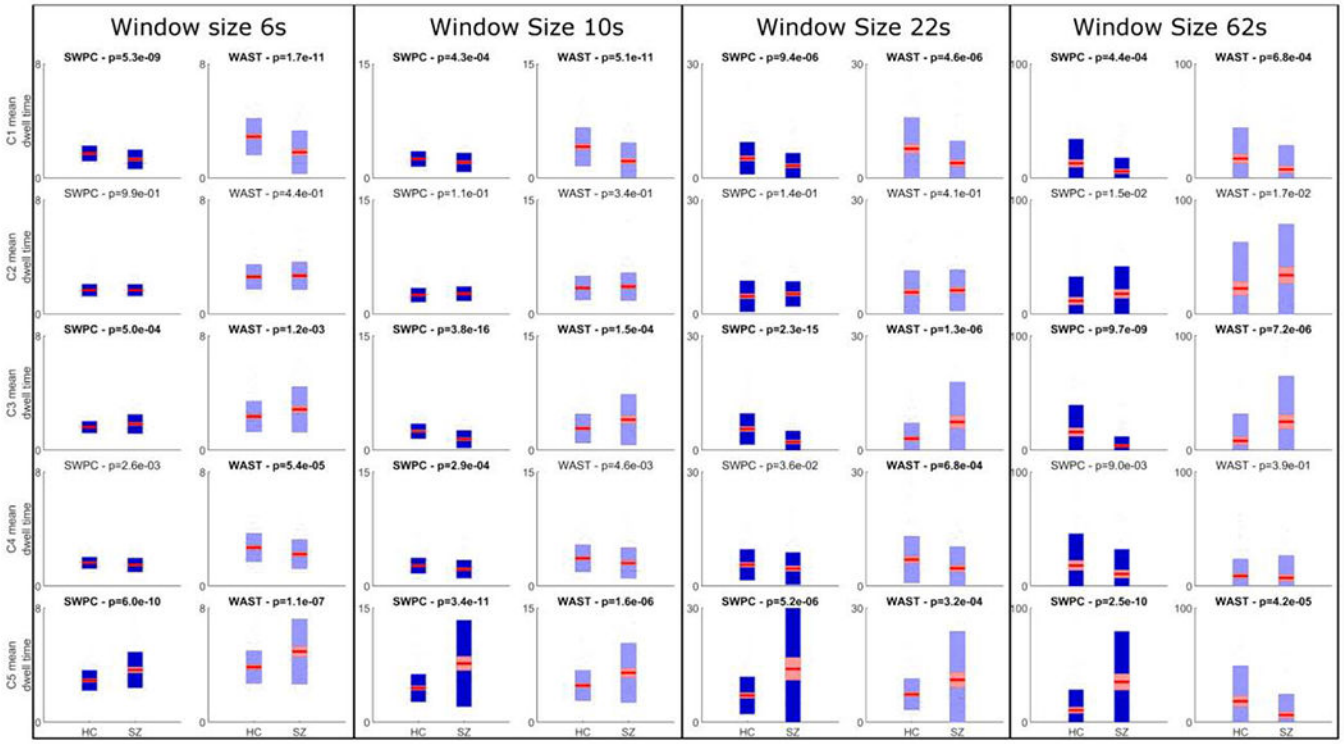

Figure 13.

mean dwell time compared between HC and SZ for different window sizes using WAST and SWPC methods. We can see here that SZ subjects tend to stay more in cluster 5 for both WAST and SWPC results. This state shows a dysconnectivity between different parts of the brain that has been reported in some previous studies. In contrast, HC subjects tend to stay more in SWPC cluster 1 and 3 and cluster 1 of WAST which shows a strong connection between AUD, VIS and SM domains. One connectivity pattern exclusive to the WAST method is only seen in cluster 3 of WAST (see Figure 11). This cluster shows a negative connectivity between motor and sensory domains that is not present in any other cluster using SWPC method. In the current figure, we see that SZ individuals tend to stay significantly longer in this state compared to HC.